

Poly ether keton keton polymer deposition on laser surface structured commercial pure titanium using magnetron sputtering

Deposição de polímero de poliéter cetona cetona em titânio comercial puro com superfície estruturada a laser usando pulverização catódica por magnetron

Aseel Mohammed AL-KHAFAJI¹, Moamin I. ISSA¹, Fatimah J. ISMAEL², Thekra Ismael HAMAD¹, Hikmat J. ALJUDY¹

1 - University of Baghdad, College of Dentistry, Department of Prosthodontics. Baghdad, Iraq.

2 - University of Baghdad, College of Dentistry, Department of Oral Diagnosis. Baghdad, Iraq.

How to cite: Al-Khafaji AM, Issa MI, Ismael FJ, Hamad TI, Aljudy HJ. Poly ether keton keton polymer deposition on laser surface structured commercial pure titanium using magnetron sputtering. *Braz Dent Sci.* 2024;27(2):e4234. <https://doi.org/10.4322/bds.2024.e4234>

ABSTRACT

Objective: This study aimed to evaluate the effect of coating titanium (Ti) dental implant with polyether ketone ketone (PEKK) polymer using magnetron sputtering on osseointegration, trying to overcome some of the problems associated with Ti alloys. **Material and Methods:** Implants were prepared from grade (II) commercially pure titanium (CP Ti), then laser was used to induce roughness on the surface of Ti. PEKK was deposited on the surface of Ti implants by radiofrequency (RF) magnetron sputtering technique. The implants were divided in to three groups: without coating (Ls), with PEKK coating using argon (Ar) as sputtering gas (Ls-PEKK-Ar), and with PEKK coating using nitrogen (N) as sputtering gas (Ls-PEKK-N). All the implants were implanted in the femoral bones of rabbits. After three different healing periods (2, 6, and 12 weeks) the rabbits were sacrificed for a mechanical examination (removal torque) and for histological examination. **Results:** The results revealed a significant increase in the removal torque mean values when using PEKK coating on Ti implants, with the highest value recorded by Ls-PEKK-N group. Histologically, the study demonstrated the progression of osteogenesis during all the research periods. It was observed that the Ls-PEKK-N group had the highest percentage of new bone formation in all healing periods. **Conclusion:** The use of PEKK as coating material on the surface of Ti implants by RF- magnetron sputtering results in an increase in the torque required to remove implants and enhance bony tissue formation around the implants especially when using nitrogen as a sputtering gas.

KEYWORDS

Dental implant; Magnetron sputtering; Osseointegration; PEKK; Titanium.

RESUMO

Objetivo: Este estudo teve como objetivo avaliar o efeito do revestimento de implante dentário de titânio (Ti) com polímero de poliéter cetona cetona (PEKK) usando pulverização catódica por magnetron na osseointegração, tentando superar alguns dos problemas associados às ligas de Ti. **Material e Métodos:** Os implantes foram preparados a partir de titânio comercialmente puro grau (II) (CP Ti), em seguida o laser foi utilizado para induzir rugosidade na superfície do Ti. PEKK foi depositado na superfície de implantes de Ti pela técnica de pulverização catódica por radiofrequência (RF). Os implantes foram divididos em três grupos: sem revestimento (Ls), com revestimento de PEKK utilizando argônio (Ar) como gás de pulverização catódica (Ls-PEKK-Ar) e com revestimento de PEKK utilizando nitrogênio (N) como gás de pulverização catódica (Ls-PEKK -N). Todos os implantes foram implantados em ossos femorais de coelhos. Após três períodos de cicatrização diferentes (2, 6 e 12 semanas), os coelhos foram sacrificados para exame mecânico (torque de remoção) e exame histológico. **Resultados:** Os resultados revelaram um aumento significativo nos valores médios do torque de remoção quando se utilizou o revestimento de PEKK em implantes de Ti, sendo o maior valor registrado pelo grupo Ls-PEKK-N. Histologicamente, o estudo demonstrou a progressão da osteogênese durante todos os períodos da pesquisa.

Observou-se que o grupo Ls-PEKK-N apresentou maior percentual de neoformação óssea em todos os períodos de cicatrização. **Conclusão:** O uso de PEKK como material de revestimento na superfície de implantes de Ti por pulverização catódica RF-magnetron resulta em um aumento no torque necessário para remover os implantes e melhorar a formação de tecido ósseo ao redor dos implantes, especialmente quando se utiliza nitrogênio como gás de pulverização catódica.

PALAVRAS-CHAVE

Implante dentário; Pulverização catódica por magnetron; Osseointegração; PEKK; Titânio.

INTRODUCTION

Dental implants have emerged as a secure and dependable therapeutic approach for those experiencing diminished dentition [1]. Titanium and its alloys are the materials that can be considered to be the most widely used for endosseous implants in dentistry, this could be due to their favorable mechanical characteristics, superior biological compatibility, and improved durability against corrosion [2]. Despite its widespread use, the use of titanium and its alloys as dental implants may be associated with a few drawbacks. One such disadvantage is the discrepancy in elastic moduli between the titanium implant and the adjacent bony tissue. This phenomenon has the ability to elevate the likelihood of mechanical stressing of the bone, hence resulting in detrimental effects on the adjacent bone and subsequent bone loss [3,4]. The success rate of dental implants depends primarily on their ability to osseointegrate and maintain surrounding bone [5,6]. The process of osseointegration can be influenced by various variables, such as the material characteristics, surface topography, and geometry of the implant. Consequently, the optimization of osseointegration in dental implants is consistently sought after in order to get favorable outcomes in clinical practice [7]. Surface alteration of dental implants, particularly through topographical means, is well recognized as an effective approach for enhancing the biological activity of these implants [8,9]. Laser surface treatment of implants has been shown to improve osseointegration by changing titanium roughness; by formation of microscopical surface structures, increasing water absorption, and enhancement of oxide layer [10]. In addition to employing modified approaches for inducing modification on the surface of the implant, certain additive methods are also utilized like implant surface coatings [11,12]. Polymers represent important dental materials that have favorable physical, mechanical, and biocompatibility characteristics [13]. PEKK is an innovative polymer

that has piqued the interest of the researchers due to its outstanding characteristics that can be employed in a wide range of applications. In the last few years, PEKK has been progressively employed as a biomaterial due to the inherent characteristics, such as excellent biocompatibility, sufficient resistance to fracture, suitable compressive, tensile, and flexural strength, modulus of elasticity comparable to that of bone, that render it appropriate for many dental and medical applications. These may include applications in orthopedics, spinal, oral, and maxillofacial surgeries, prosthodontics, and dental implants [6,14-17]. Magnetron sputtering is one of the methods that are used for coating process. It is a physical technique for vapor deposition in which electrically charged particles strike a desired target's surface under the influence of both magnetic and electrical fields [18,19]. Several studies were conducted to implement various coating materials like calcium phosphate, hydroxyapatite, dicalcium pyrophosphate, boron nitride using magnetron sputtering technique, on the surface of dental and medical implants to exert a topographical change in an attempt to improve the osseointegration of the implants [20-24]. This study aimed to assess the mechanical and histological effects of depositing PEKK material by magnetron sputtering on laser surface textured CPTi implant screws. The null hypothesis is that the coating of laser surface textured CPTi implants with PEKK polymer doesn't affect the required torque to remove implant from the bone nor the histology of the bone in the implantation site.

MATERIALS AND METHODS

Sample preparation

A commercially pure titanium (CP Ti) grade (II) (Orotig Srl EU Company, Italy) was utilized in the form of annealed rods of 1,000 mm in length and 6 mm in diameter. These rods were

employed to fabricate 180 implant screws. A turning machine was used to create a screw-shaped specimen (implants) with dimensions of 3 mm diameter and 5 mm length. The specimens underwent an ultrasonic cleaning process with ethanol followed by distilled water then air dried. The sample size was determined by using G power 3.1.9.7 (Program written by Franz-Faul, University of Kiel, Germany) with power of study=85%, alpha error of probability=0.05 two sided, assume effect size of F is 0.4 (large effect size), and nine groups (3 groups with three different periods) thus sample size is about 90 implants (10 implants for each group in each healing period). This calculation applied for the removal torque test, and applied separately for the histological test (in which also 90 implants required). Therefore, a total of 180 implants were used [25, 26].

Surface structuring by laser

The laser was utilized to induce surface roughening on titanium. The surfaces of titanium specimens underwent structuring under ambient conditions using a pulse mode CNC fiber laser device. (Jinan JinQiang 20W laser--- China) having an output laser power of 20-Watt with an emission wavelength of 1064 nm and maximum scanning speed of 7000 mm/sec. The sample-laser source distance was 20 cm. The dot design was utilized to structure the entire surface of the specimen, with 0.01 mm space among each neighboring dot in every direction.

PEKK coating

The deposition of PEKK coatings on Ti screws was carried out using radiofrequency reactive magnetron sputtering technique and device (Torr International Inc., United States) (Figure 1), employing PEKK as the sputtering target.

The sputtering target (PEKK disc) which has (50mm) diameter and (4mm) thickness, was attached to the anode (positive charge) of system and the specimens (titanium implants) were mounted on the custom-made holder and attached to cathode (negative charge) rotating disc. The specimens to target distance has been set at 5 cm. The cathode disc was rotated at a constant velocity to provide uniform distribution of PEKK material across all surfaces of the implants. The vacuum process was initiated to remove air from the chamber of the device, ultimately achieving a base pressure of 5.5×10^{-6} mbar, and the space inside was filled with either argon gas or nitrogen gas. A preliminary sputtering process was conducted at an operating pressure of 1.5×10^{-3} mbar to cleanse the surface of the target and establish stable sputtering circumstances.

After setting the specimens' temperature to 60C for one hour, and the operational power equaled 50 watt a thin coating of PEKK was produced (Figure 2).

The implant screws preparation workflow is shown in (Figure 3).

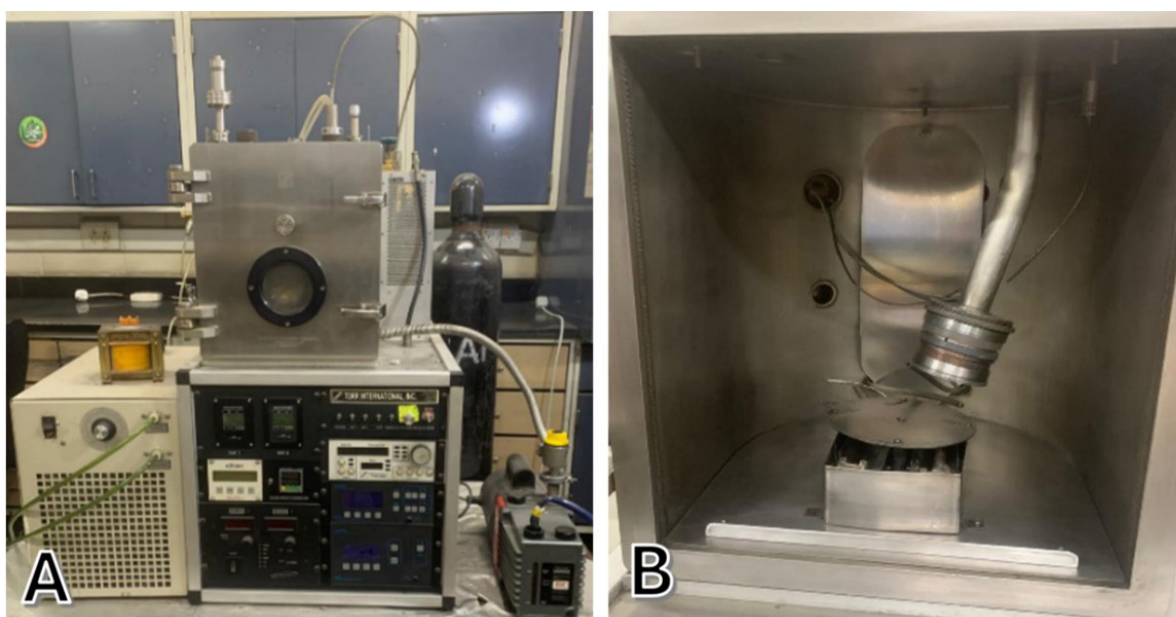


Figure 1 - Magnetron sputtering device, (A) The entire apparatus; (B) Sputtering chamber.

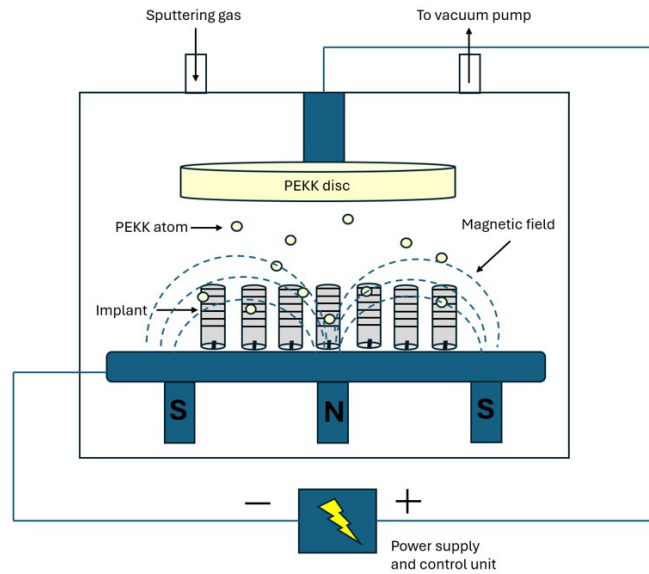


Figure 2 - Schematic illustration of magnetron sputtering process.

Elemental analysis with EDX

Energy dispersive X-ray analysis (EDX) was performed to determine the composition information and elemental identification of the implant surface. This was accomplished by using field-emission scanning electron microscope with EDX system attachment (MIRA3, TESCAN, Czech Republic).

Sterilization of the specimens

All the specimens (implants) were sterilized using autoclave due to the PEKK materials' ability to endure elevated temperatures and their compatibility with steam sterilization [27,28].

Sample grouping

According to the type of surface modification the titanium screws were divided into 3 groups:

Ls: CP Ti screws with laser structuring and without coating;

Ls-PEKK-Ar: CP Ti screws with laser structuring and PEKK coating using argon gas in RF-magnetron sputtering;

Ls-PEKK-N: CP Ti screws with laser structuring and PEKK coating using nitrogen gas in RF-magnetron sputtering.

These groups were tested mechanically (removal torque) and histologically (histomorphometric analysis) on three different healing periods (2, 6, and 12 weeks). A total of

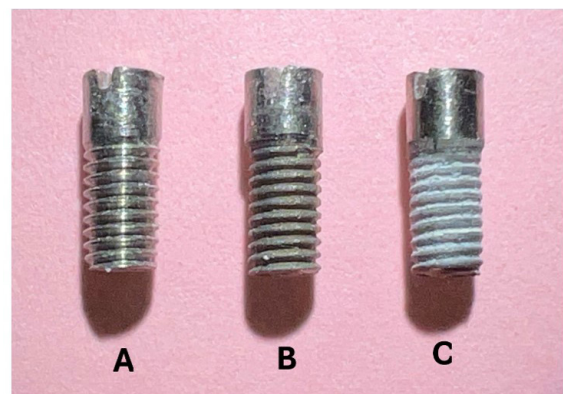


Figure 3 - Ti implant screws preparation workflow, (A) Before surface structuring by laser; (B) After laser structuring; (C) After PEKK coating.

180 implant screws were used, with 10 screws being given to each group for each test during each healing period.

A diagrammatic flowchart of sample preparation and the entire workflow is shown in (Figure 4).

Animal experiment (in vivo study)

This study was approved by the Research Ethics Committee of the College of Dentistry, University of Baghdad (ref. number 244, project number 244221 at 10.2.2021). A total of sixty healthy New Zealand white rabbits aged 10 to 12 months and weighing 2–2.5 kg, without any apparent illnesses, were chosen for the study. The animals were maintained in a controlled

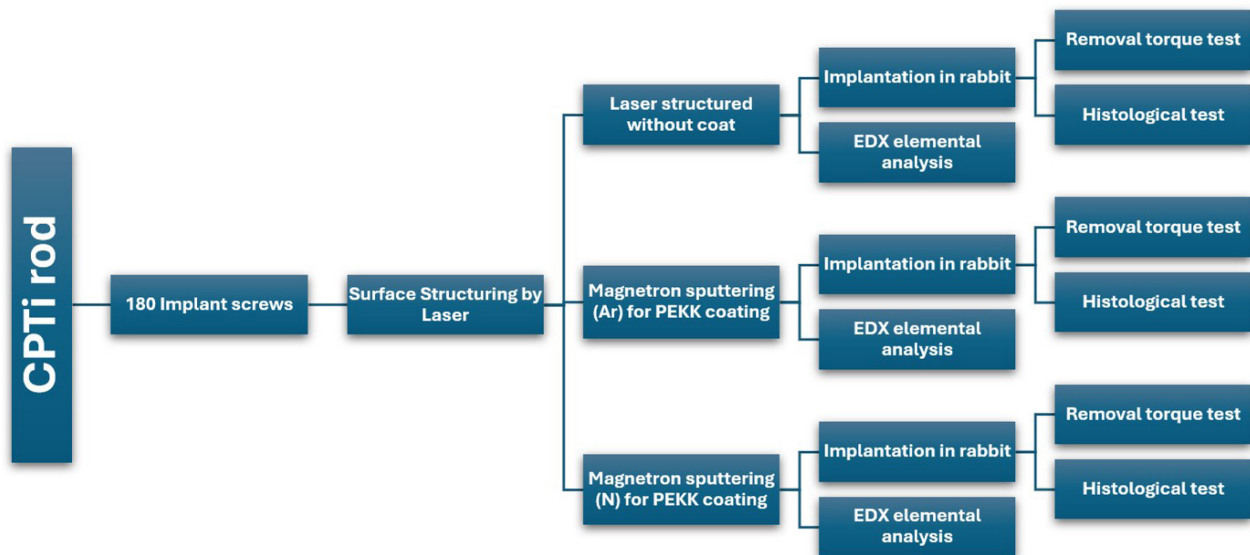


Figure 4 - A diagrammatic flowchart of the entire workflow.

environment, conforming to conventional parameters, with a regulated temperature range of 23°C–25°C., as well as dietary needs supplies. The study's rabbits were divided randomly into three groups based on healing period: 2 weeks, 6 weeks, and 12 weeks. A simple randomization method was used. The rabbits and the samples were randomly coded and numbered (to allow later data interpretation after data analysis), and the rabbits were randomly distributed all over the three healing periods for the mechanical (removal torque) and histological tests. However, for organization purposes and to facilitate later data interpretation three implants were implanted in the femoral bones in each rabbit (the right femur received 1 implant from Ls group, while the left femur received 2 implants 1 from Ls-PEKK-Ar group and 1 from Ls-PEKK-N group, ensuring 1cm distance between the two implants which allow independency of each implant and implant site). Each primary group has 20 animals; 10 had to be sacrificed for histological examination and 10 for mechanical testing using a removal torque test, and this was applied for each healing period.

Surgical procedure

The surgical procedure was conducted using a meticulous and extremely sterile aseptic method. The rabbits were anaesthetized with an intramuscular injection of ketamine hydrochloride 50 mg at a dosage of 1 ml/ kg, along with xylocaine 2% at a dosage of 1 ml /kg of body weight. After surgery, 0.05 mg/kg buprenorphine was injected intramuscularly to alleviate pain.

Continuous monitoring of the animal's body temperature and oxygen levels was performed throughout the surgical procedure. The operative site was prepared through the removal of fur and subsequent disinfection of the skin using 70% ethanol and chlorhexidine then surgical towels and iodine-ethanol wash were applied.

The lateral side of the femoral bone was exposed by making approximately a 3cm incision then a flap and skin were carefully reflected after gaining access to the bone a guiding drill was used, the initial holes (1.8 mm in diameter, 5 mm in depth, and 1 cm apart from each other) were made using an implant operation engine and drills (Dentium F28D104 112, Korea). The drilling speed was 800 rpm, and the torque was 20 N accompanied with saline irrigation. The implant bed was gradually enlarged in a stepwise manner up to a diameter of 2.8 mm. Afterwards, the implant bed was thoroughly washed of drilling debris utilizing a solution of normal saline. Following this, the sterilized implant was taken from its packaging and then screwed into the designated site employing a screwdriver then torqued using torque meter to 10 N.cm [29,30]. The surgical wound was stitched and disinfected using iodine and treated with a local oxytetracycline spray then covered with sterile gauze, which was changed on a daily basis. Additionally, a systemic oxytetracycline injection at a dosage of 20% and 0.5ml /kg was administered each day for a duration of five days.

After surgery, rabbits and the surgical site are regularly checked for infections and concerns.

The animals were subjected to supervision for durations of 2 weeks, 6 weeks, and 12 weeks.

Removal torque test

For each healing interval (2, 6, and 12 weeks), ten rabbits were employed for removal torque mechanical testing. The rabbits were subjected to anesthesia, following which an incision in the lateral side of the rabbit femur was made then the muscles and fascia were retracted to reveal the implants. The digital torque meter (Hitachi Maxwell LTD./174, Japan) was utilized to engage the slit in the implant head, enabling the recording of the maximal peak torque required for loosening the implant from the bony site. The removal torque was measured in units of Newton-centimeters.

Histology and histomorphometry

Tissue sample for histological evaluation was collected by the utilization of a disc cutter connected to a slow-speed rotation handpiece, which was accompanied with robust freezing. To facilitate humane euthanasia, a surplus quantity of anesthetic solution was administered to the rabbits. The excised tissue samples were promptly immersed in a solution of 10% buffered formalin and allowed to undergo fixation for a duration of 24 hours. Subsequently, the tissues were immersed in a solution of 10% formic acid to facilitate the process of decalcification. The tissue samples were subjected to a two-week period of fixation, after which the screws were removed, rendering the specimens suitable for histological investigation.

The tissue samples underwent paraffin embedding, formalin fixation, and hematoxylin and eosin staining. Specifically, the Olympus CH model light microscope was used to examine the dyed slides. A modified adaptor called Labcam, made in the United States, was used in conjunction with an iPhone camera to capture a series of images at different magnifications.

A histomorphometric analysis was performed with the software program Image J Version 1.52. The newly formed bone's area was calculated by software using pixels. The diameter of the circular image was measured using the integrated ruler of the microscope and the Picture J program on a desktop computer to transform the pixel values into millimeter measurements (Image J analyze set scale Pixels in mm). A precise scale factor

and the magnification power used to take all the photos were calculated for the microscope.

The percentage of new bone formation area (NBFA) for each experimental group and at different points during the healing process was calculated using the formula used in this study. The calculation of the new bone formation area as a percentage of the total tissue area, denoted as NBFA%, yields a value of 100%. This approach yielded a quantification of the extent of new bone formation surrounding the implant site.

Statistical analysis

Statistical analysis of the data was carried out using Prism 8 (GraphPad Software, USA) (RRID:SCR_002798). The results were visually represented using bar charts, where the mean values were positioned within the vertical bars and the standard deviation was indicated above the bars. To determine statistical significance across groups, one-way analysis of variance (ANOVA) was used, and for multiple comparisons, Tukey's HSD (honestly significant difference) post-hoc test was used at a level of significance of 0.05.

RESULTS

Elemental analysis with EDX

The EDX spectrum and elemental analysis of all groups are presented in (Figure 5). The EDX spectrum obtained from the Ls group showed titanium (Ti) with energy at 4.5 keV and oxygen (O) with energy at 0.51 keV. While the spectrum from Ls-PEKK-Ar group showed carbon (C) with energy at 0.25 KeV in addition to both (Ti) and (O). Furthermore, the spectrum from Ls-PEKK-N group showed titanium, oxygen, carbon and nitrogen (N) with energy at 0.39 keV.

Removal torque test

The results were visually represented using a bar chart, where the torque mean values were positioned within the vertical bars and the standard deviation was indicated above the bars (Figure 6). During the three healing periods (2, 6, and 12 weeks) statistical analysis using one way ANOVA showed a significant difference in torque required to remove the implant among the groups ($P < 0.0001$). Multiple comparisons using the Tukey's HSD test among the groups of each healing period showed a significant differences

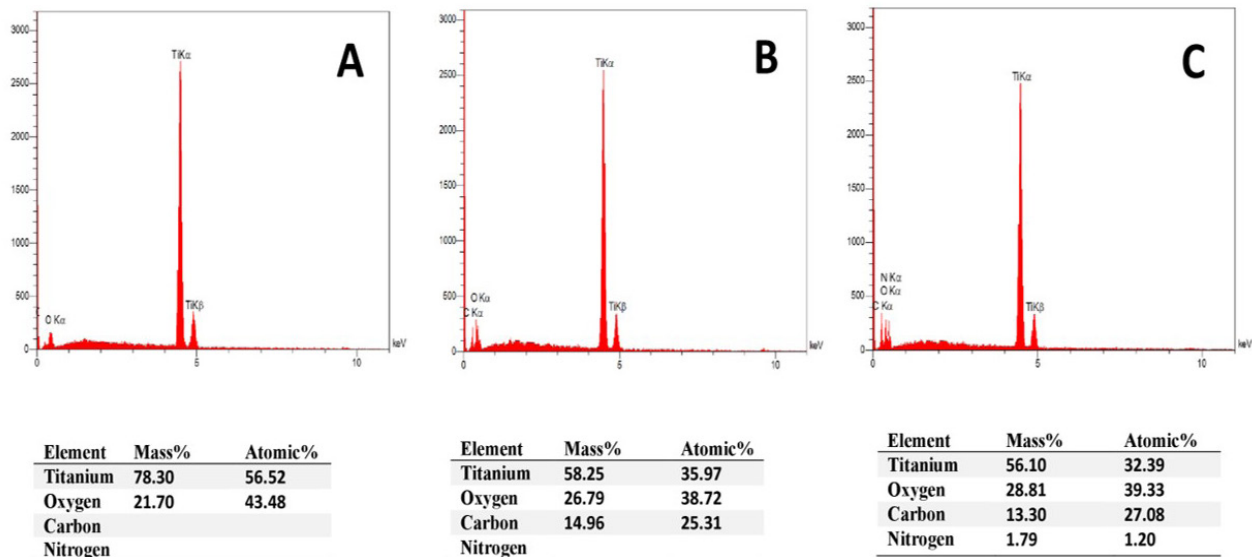


Figure 5 - EDX results of (A) Ls implant; (B) Ls-PEKK-Ar implant, and (C) Ls-PEKK-N implant.

among them ($P < 0.0001$), except for the 2 weeks period where there was non-significant difference between Ls-PEKK-Ar group and Ls-PEKK-N group ($P = 0.1857$). The highest torque mean value recorded by Ls-PEKK-N group in all periods, for 2 weeks (20.13 ± 1.31) while for 6 weeks (42.98 ± 0.95) and for 12 weeks (65.25 ± 0.78) (Figure 6). So, the outcomes of the removal torque test were recorded an increase in the torque required for implant removal with the use of PEKK as coating.

Histology and histomorphometry

Histological analysis conducted at different stages of the healing process revealed the progression of osteogenesis in the experimental cohorts as shown in (Figure 7).

The Ls group had minimal new bone formation after a 2-week period, presented as dispersed immature bone trabeculae surrounding the implant space as depicted in Figure 8A, with an estimated area of 2.18%. On the other hand, it was observed that the Ls-PEKK-N group had the highest percentage of new bone formation (2.91%) during this period, whereas the Ls-PEKK-AR group showed a greater level of new bone development (2.63%). The histological sections revealed woven bone trabeculae that were encircled by osteoblasts that were actively functioning. Figure 8B, C.

At the 6-week time point, it can be observed that all groups had a greater extent of new bone formation, this was characterized by the presence

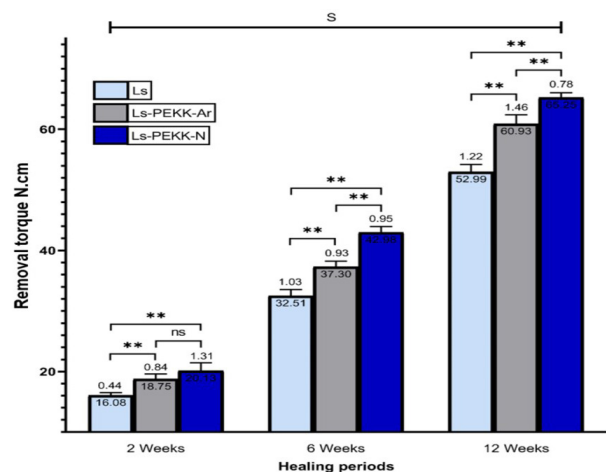


Figure 6 - Removal torque mean values with standard deviation, and the level of significance between the groups in at 2,6 and 12-week healing intervals (ns: non-significant, **: significant difference).

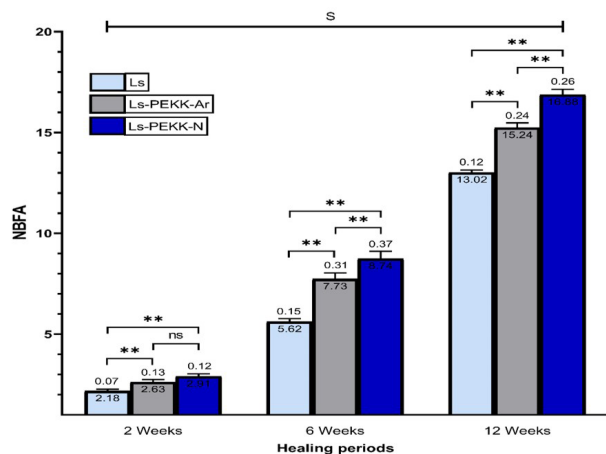


Figure 7 - NBFA with standard deviation, and the level of significance between the groups in at 2,6 and 12 week healing intervals (ns: non-significant, **: significant difference).

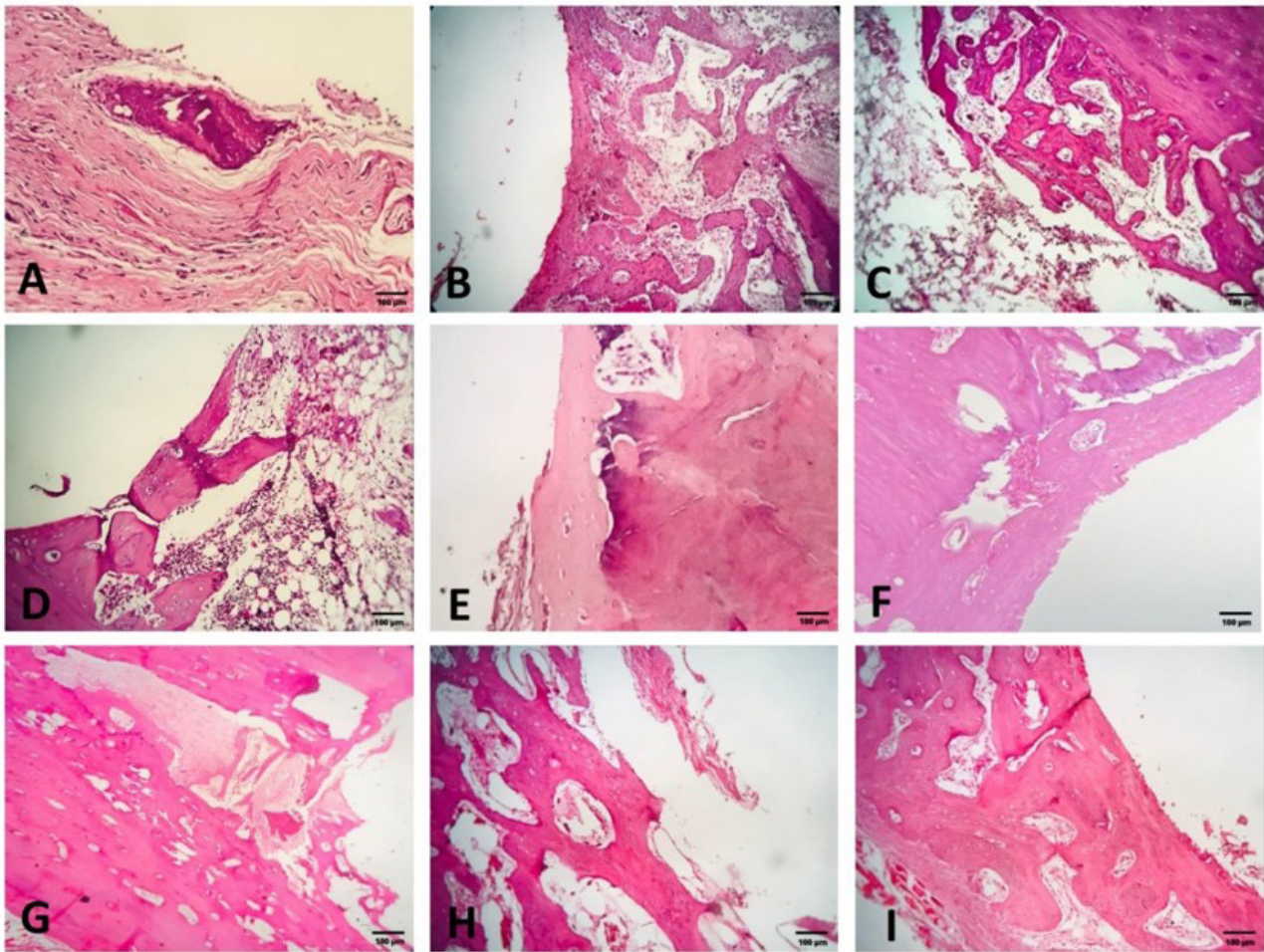


Figure 8 - Hematoxylin and eosin cross sectional histological view of new bone formation area surrounding implant space (4X), (A) control group at 2-week; (B) Ls-PEKK-AR at 2-week; (C) Ls-PEKK-N group at 2-week; (D) control group at 6-weeks; (E) Ls-PEKK-AR at 6 weeks; (F) Ls-PEKK-N group at 6 weeks; (G) control group at 12 weeks; (H) Ls-PEKK-AR at 12 weeks; (I) Ls-PEKK-N group at 12 weeks.

of more developed woven bone trabeculae, as well as prominent functioning osteoblastic rim and osteocytes inside the lacunae as shown in Figure 8D, E, F. Among the groups, it was observed that the Ls-PEKK-N group had the highest percentage of new bone production, measuring at 8.74% and the most mature looking bone trabeculae.

After a duration of 12 weeks, it was seen that all groups exhibited notable enhancements in bone formation and maturation, as shown in Figure 8G, H, I. The Ls group had a substantial increase in new bone formation (13.02%), accompanied by a considerable presence of osteoblasts and osteocytes, as well as the development of Haversian networks. The PEKK-AR group had a comparatively elevated rate of new bone formation at 15.24%. Conversely, the PEKK-N group, characterized by advanced maturity, well-structured Haversian systems, and significant lamellar bone organization,

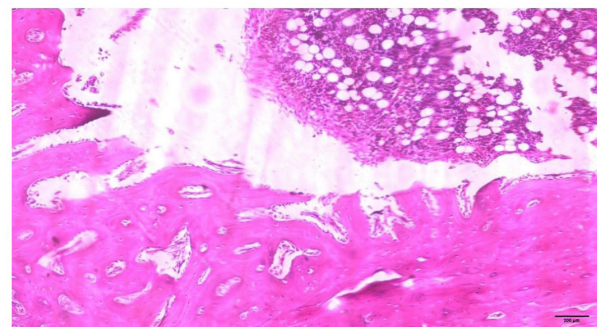


Figure 9 - A histological image in panoramic view for the bone-implant space interface at 10X magnification.

demonstrated the highest rate of new bone formation at 16.88%.

A histological image in panoramic view for the bone-implant space interface showing bone formation in screw threads area using Lecia inverted light microscope at 10X magnification (Figure 9).

DISCUSSION

Surface modification of dental implants, particularly by alterations in topography and chemical structures, has been recognized as a highly successful approach for enhancing the bioactivity of these implants [8,9,31]. In addition to that stress distribution of occlusal load to the peripheral bone surrounding dental implants is crucial for implant longevity [32].

PEKK exhibits exceptional physical as well as mechanical characteristics [17]. PEKK's durability, shock absorption, sufficient strength (65 MPa), and fracture resistant features make it a viable restorative material. When compared to dentin, the PEKK has a similar compressive strength but a lower modulus of elasticity. PEKK, like polyetheretherketone (PEEK), has an elastic modulus that is similar to that of bone. Therefore, it can be concluded that PEKK possesses desirable mechanical characteristics and excellent stress distribution, making it a suitable biomaterial for dental implants [33,34].

In the present study RF- magnetron sputtering technique, was used for coating laser textured Ti dental implants with PEKK material, in an attempt to enhance the implant bioactivity and improve osseointegration that was evaluated by measuring the torque required to remove implants from bone and by histological evaluation [35,36]. According to the findings of the current study, coating laser textured Ti dental implants with PEKK polymer resulted in an increase in removal torque and in bone formation and maturation. Therefore, the null hypothesis was rejected.

In this study the healing periods were selected based on different studies. Different studies used different periods (one or more) whether 2, 4, 6, 8, or 12 weeks. In this study we used 2 weeks as the first period which was the first period used in many studies [37-39] and it was noted that a new bone formation surrounding the dental implant was evident 2 weeks after implant insertion [37]. While in a study by Dhaliwal et al., 2017 rabbits were sacrificed after 6 weeks healing period [40]. Also, Gehrke and Marin, 2015 used 6 weeks as the first euthanasia period [41]. The 12 weeks healing period was the longest used in most of the studies [37,41,42], in which considerable direct bone contact with the implant was observed after 12 weeks [37].

The results of this study showed that the removal torque mean values for all the groups were increased over time. This elevation in torque mean value with time might be due to progressive bone formation and the maturation of woven bone to lamellar bone around the implants that consequently improved osseointegration and the mechanical capacity with time [43,44].

The results of this study showed that coating Ti dental implant with PEKK results in greater removal torque mean values. Although laser surface treatment causes increase in the osseointegration capability of the dental implant, which might be due to increase in the implant surface roughness [45,46]. However, coating implant with PEKK resulted in stronger osseointegration capability that could be attributed to the greater surface roughness that related to particle size of PEKK powder and change of the surface chemistry.

Regarding chemistry and surface microstructure, a research reported that PEKK has a large number of ketone groups which enhance the capacity for surface chemical modification that can result in complicated surface topography, increased surface area, and a microrough surface, all of which can enhance cellular activity and the process of osteointegration on the surface of PEKK [47,48].

Histological and histomorphometric analysis of this study revealed a significant increase in NBFA with highly organized bone trabeculae surrounded by well-defined osteoblastic rim around the implant site in all groups comparative to Ls group and this result may be related to many factors, the first one is the increase in the implant roughness that led to increase contact area, cell adhesion, proliferative abilities, interlocking with the tissue that enhance implants osseointegration [46,49,50]. The rough surfaces had confirmed superior biomolecules adsorption from biological fluids, which has the probability to modify the events cascade that leads to intimate bone apposition and bone healing with the implants [51,52].

Regarding the differences in the mean values of torque removal between Ls-PEKK-N and Ls-PEKK-Ar groups, although argon is the preferred operating gas for magnetron sputtering procedures because of its substantial atomic mass, unreactive nature, and comparatively affordable price. Different gases can be utilized for sputtering deposition, each

with different mass properties. Consequently, the momentum behavior varies when solid surfaces are bombarded by ions, which in turn affects the sputtering yield, particle implantation, and inclusion of process gas into the formed coatings. The gas incorporation in the coating is higher for sputtering gases with lower atomic mass [53].

Due to the fact that nitrogen has a lower atomic mass than argon, so this can explain the result of EDX analysis which showed the presence of nitrogen in the Ls-PEKK-N group (Figure 5). Nitrogen-containing compounds have the ability to influence arginylglycylaspartic acid; this is the primary integrin binding domain to fibronectin and a member of the adhesive protein class. It has been proposed that extracellular fibronectin and cell adhesion are strongly linked. Therefore, functional groups that include nitrogen (which presented on implant surface) may have the ability to modulate the integrin-mediated signaling cascade, which in turn promotes adhesion, growth, and differentiation of osteoblast cells [54]. In addition to that the negative charge of osteoblast cells may interact with the positive charge of the functional groups that contain nitrogen facilitating cell adhesion and promoting cell growth and the development of bone tissue [55,56]. We Hypothesize that these mechanisms may explain the higher mean value of torque removal and the highly significant increase in NBFA and mature looking bone trabeculae of Ls-PEKK-N group in comparison to Ls-PEKK-Ar group.

CONCLUSION

Coating Ti dental implants with PEKK polymer by RF-magnetron sputtering can result in an improved stability of implants that can be concluded from a higher torque required to remove implant from bone and from histomorphometric analysis which revealed an increase in NBFA and mature-looking bone trabeculae, especially when using nitrogen as sputtering gas. These findings open up new research avenues for utilizing these new technologies to improve osteointegration around the implant site.

Author's Contributions

AMAK: Conceptualization, Methodology, Investigation, Resources, Data Curation, Supervision, Project Administration and Funding

Acquisition. MII: Conceptualization, Software, Writing – Original Draft Preparation, Writing – Review & Editing, Visualization and Funding Acquisition. FJI: Methodology, Software, Validation, Formal Analysis, Investigation, Resources, Data Curation, Writing – Original Draft Preparation. TIH: Conceptualization, Validation, Formal Analysis, Visualization, Supervision, Project Administration and Funding Acquisition. HJA: Validation, Formal Analysis, Investigation, Resources, Visualization, Supervision, Project Administration and Funding Acquisition.

Conflict of interest

The authors have no proprietary, financial, or other personal interest of any nature or kind in any product, service, and/or company that is presented in this article.

Funding

This research did not receive any specific grant from funding agencies in the public, commercial, or not-for-profit sectors.

Regulatory Statement

This study was conducted in accordance with all the provisions of the local human subjects oversight committee guidelines and policies of the research ethics committee of the college of dentistry, university of Baghdad. The approval code for this study is (ref. number 244, project number 244221 at 10.2.2021).

REFERENCES

1. Henningsen A, Smeets R, Köppen K, Sehner S, Kornmann F, Gröbe A, et al. Immediate loading of subcrestally placed dental implants in anterior and premolar sites. *J Craniomaxillofac Surg.* 2017;45(11):1898-905. <http://doi.org/10.1016/j.jcms.2017.08.017>. PMID:28935490.
2. Renouard F, Nisand D. Impact of implant length and diameter on survival rates. *Clin Oral Implants Res.* 2006;17(Suppl 2):35-51. <http://doi.org/10.1111/j.1600-0501.2006.01349.x>. PMID:16968380.
3. Nagasawa M, Takano R, Maeda T, Uoshima K. Observation of the bone surrounding an overloaded implant in a novel rat model. *Int J Oral Maxillofac Implants.* 2013;28(1):109-16. <http://doi.org/10.11607/jomi.2388>. PMID:23377055.
4. Al-Khafaji AM, Hamad TI. Surface analysis of the PEKK coating on the CP Ti implant using laser technique. *Int J Med (Dubai).* 2021;28(1):29-32. <http://doi.org/10.1155/2023/7840601>.
5. Moraes MB, de Toledo VGL, Nascimento RD, Gonçalves FCP, Raldi FV. Evaluation of implant osseointegration success: retrospective

- study at update course. *Braz Dent Sci.* 2015;18(4):98-103. <http://doi.org/10.14295/bds.2015.v18i4.1157>.
6. Najeeb S, Bds ZK, Bds SZ, Bds MS. Bioactivity and Osseointegration of PEEK Are Inferior to Those of Titanium: A Systematic Review. *J Oral Implantol.* 2016;42(6):512-6. <http://doi.org/10.1563/aid-joi-D-16-00072>. PMID:27560166.
 7. Zafar MS, Fareed MA, Riaz S, Latif M, Habib SR, Khurshid Z. Customized therapeutic surface coatings for dental implants. *Coatings.* 2020;10(6):568. <http://doi.org/10.3390/coatings10060568>.
 8. Fernandes VVB Jr, da Rosa PAA, Grisante LAD, Embacher FC, Lopes BB, de Vasconcellos LGO, et al. Argon plasma application on the surface of titanium implants: osseointegration study. *Braz Dent Sci.* 2023;26(4):e3843. <http://doi.org/10.4322/bds.2023.e3843>.
 9. Mandracci P, Mussano F, Rivolo P, Carossa S. Surface treatments and functional coatings for biocompatibility improvement and bacterial adhesion reduction in dental implantology. *Coatings.* 2016;6(1):7. <http://doi.org/10.3390/coatings6010007>.
 10. Simões IG, Dos Reis AC, da Costa Valente ML. Analysis of the influence of surface treatment by high-power laser irradiation on the surface properties of titanium dental implants: a systematic review. *J Prosthet Dent.* 2023;129(6):863-70. <http://doi.org/10.1016/j.prosdent.2021.07.026>. PMID:34493390.
 11. Dong H, Liu H, Zhou N, Li Q, Yang G, Chen L, et al. Surface modified techniques and emerging functional coating of dental implants. *Coatings.* 2020;10(11):1012. <http://doi.org/10.3390/coatings10111012>.
 12. Refaat MM, Hamad TI. Evaluation of mechanical and histological significance of nano hydroxyapatite and nano zirconium oxide coating on the osseointegration of CP Ti implants. *J Bagh Coll Dent.* 2016;28(3):30-7. <http://doi.org/10.12816/0031105>.
 13. Xu X, He L, Zhu B, Li J, Li J. Advances in polymeric materials for dental applications. *Polym Chem.* 2017;8(5):807-23. <http://doi.org/10.1039/C6PY01957A>.
 14. Alqurashi H, Khurshid Z, Syed AUY, Rashid Habib S, Rokaya D, Zafar MS. Polyetherketoneketone (PEKK): an emerging biomaterial for oral implants and dental prostheses. *J Adv Res.* 2021;28:87-95. <http://doi.org/10.1016/j.jare.2020.09.004>. PMID:33384878.
 15. Stawarczyk B, Jordan P, Schmidlin PR, Roos M, Eichberger M, Gernet W, et al. PEEK surface treatment effects on tensile bond strength to veneering resins. *J Prosthet Dent.* 2014;112(5):1278-88. <http://doi.org/10.1016/j.prosdent.2014.05.014>. PMID:24969411.
 16. Fuhrmann G, Steiner M, Freitag-Wolf S, Kern M. Resin bonding to three types of polyaryletherketones (PAEKs)-durability and influence of surface conditioning. *Dent Mater.* 2014;30(3):357-63. <http://doi.org/10.1016/j.dental.2013.12.008>. PMID:24461250.
 17. Fayad NMEH, Bahig DE. The effect of different framework's material on strain induced in distal abutment in mandibular Kennedy's class II: an in-vitro study. *Braz Dent Sci.* 2023;26(3):e3775. <http://doi.org/10.4322/bds.2023.e3775>.
 18. Ma C, Zhao C, Fan X, Liu Z, Liu J. Preparation of non-stoichiometric Al₂O₃ film with broadband antireflective by magnetron sputtering. *Chem Phys Lett.* 2021;v:138299. <http://doi.org/10.1016/j.cplett.2020.138299>.
 19. Safi IN, Hussein BMA, Aljudy HJ, Tukmachi MS. Effects of long durations of rf-magnetron sputtering deposition of hydroxyapatite on titanium dental implants. *Eur J Dent.* 2021;15(3):440-7. <http://doi.org/10.1055/s-0040-1721314>. PMID:33511600.
 20. Yokota S, Nishiwaki N, Ueda K, Narushima T, Kawamura H, Takahashi T. Evaluation of thin amorphous calcium phosphate coatings on titanium dental implants deposited using magnetron sputtering. *Implant Dent.* 2014;23(3):343-50. <http://doi.org/10.1097/ID.000000000000098>. PMID:24819811.
 21. Akhtar M, Uzair S, Rizwan M, Ur Rehman MA. The improvement in surface properties of metallic implant via magnetron sputtering: recent progress and remaining challenges. *Front Mater.* 2022;8:747169. <http://doi.org/10.3389/fmats.2021.747169>.
 22. Yonggang Y, Wolke JG, Yubao L, Jansen JA. In vitro evaluation of different heat-treated radio frequency magnetron sputtered calcium phosphate coatings. *Clin Oral Implants Res.* 2007;18(3):345-53. <http://doi.org/10.1111/j.1600-0501.2006.01332.x>. PMID:17298487.
 23. Hung K-Y, Lai H-C, Feng H-P. Characteristics of RF-Sputtered Thin Films of Calcium Phosphate on Titanium Dental Implants. *Coatings.* 2017;7(8):126. <http://doi.org/10.3390/coatings7080126>.
 24. Gökmenoğlu CEREN, Özmeriç N, Çakal G, Dökmetaş N, Ergene C, Kaftanoğlu B. Coating of titanium implants with boron nitride by RF-magnetron sputtering. *Bull Mater Sci.* 2016;39(5):1363-70. <http://doi.org/10.1007/s12034-016-1273-0>.
 25. Cohen J. *Statistical power analysis for the behavioral sciences* 2nd ed. Hillsdale: L. Erlbaum Associates; 1988.
 26. Faul F, Erdfelder E, Buchner A, Lang A-G. Statistical power analyses using G* Power 3.1: tests for correlation and regression analyses. *Behav Res Methods.* 2009;41(4):1149-60. <http://doi.org/10.3758/BRM.41.4.1149>. PMID:19897823.
 27. Godara A, Raabe D, Green S. The influence of sterilization processes on the micromechanical properties of carbon fiber-reinforced PEEK composites for bone implant applications. *Acta Biomater.* 2007;3(2):209-20. <http://doi.org/10.1016/j.actbio.2006.11.005>. PMID:17236831.
 28. Verma A. Novel innovations in dental implant biomaterials science: zirconia and PEEK polymers. *Int J Appl Dent Sci.* 2018;4(4):25-9.
 29. Togni F, Baras F, Ribas Mde O, Taha MO. Histomorphometric analysis of bone tissue repair in rabbits after insertion of titanium screws under different torque. *Acta Cir Bras.* 2011;26(4):261-6. <http://doi.org/10.1590/S0102-86502011000400003>. PMID:21808837.
 30. Medina CEB, Rafael CF, Volpato CAM, Özcan M, de Vasconcelos DK. Evaluation of removal torque values for titanium screws of prosthetic abutments after different torque application techniques: in vitro study. *Braz Dent Sci.* 2016;19(4):12-8. <http://doi.org/10.14295/bds.2016.v19i4.1295>.
 31. Muna N, Rahman HA. Mechanical Evaluation of Pure Titanium Dental Implants Coated with a Mixture of Nano Titanium Oxide and Nano Hydroxyapatite. *J Bagh Coll Dent.* 2016;28(3):38-43. <http://doi.org/10.12816/0031106>.
 32. Inci SD, Turp V, Tuncelli FB. Stress distribution in peri-implant bone, implants, and prostheses: 3D-FEA of marginal bone loss and prosthetic design. *Braz Dent Sci.* 2024;27(2):e4168. <http://doi.org/10.4322/bds.2024.e4168>.
 33. Schwitalla AD, Spintig T, Kallage I, Müller WD. Flexural behavior of PEEK materials for dental application. *Dent Mater.* 2015;31(11):1377-84. <http://doi.org/10.1016/j.dental.2015.08.151>. PMID:26361808.
 34. Song CH, Choi JW, Jeon YC, Jeong CM, Lee SH, Kang ES, et al. Comparison of the Microtensile Bond Strength of a Polyetherketoneketone (PEKK) Tooth Post Cemented with Various Surface Treatments and Various Resin Cements. *Materials (Basel).* 2018;11(6):916. <http://doi.org/10.3390/ma11060916>. PMID:29844270.
 35. Chang PC, Lang NP, Giannobile WV. Evaluation of functional dynamics during osseointegration and regeneration associated with oral implants. *Clin Oral Implants Res.* 2010;21(1):1-12. <http://doi.org/10.1111/j.1600-0501.2009.01826.x>. PMID:20070743.

36. Atsumi M, Park SH, Wang HL. Methods used to assess implant stability: current status. *Int J Oral Maxillofac Implants*. 2007;22(5):743-54. PMID:17974108.
37. Mori H, Manabe M, Kurachi Y, Nagumo M. Osseointegration of dental implants in rabbit bone with low mineral density. *J Oral Maxillofac Surg*. 1997;55(4):351-61, discussion 62. [http://doi.org/10.1016/S0278-2391\(97\)90124-5](http://doi.org/10.1016/S0278-2391(97)90124-5). PMID:9120698.
38. Soto-Peñaloza D, Caneva M, Viña-Almunia J, Martín-de-Llano JJ, Peñarrocha-Oltra D, Peñarrocha-Diago M. Bone-healing pattern on the surface of titanium implants at cortical and marrow compartments in two topographic sites: an experimental study in rabbits. *Materials (Basel)*. 2019;12(1):85. <http://doi.org/10.3390/ma12010085>. PMID:30591652.
39. Jinno Y, Stocchero M, Galli S, Toia M, Becktor JP. Impact of a hydrophilic dental implant surface on osseointegration: biomechanical results in rabbit. *J Oral Implantol*. 2021;47(2):163-8. <http://doi.org/10.1563/aaid-joi-D-19-00217>. PMID:32663272.
40. Dhaliwal JS, Albuquerque RF Jr, Murshed M, Feine JS. Osseointegration of standard and mini dental implants: a histomorphometric comparison. *Int J Implant Dent*. 2017;3(1):15. <http://doi.org/10.1186/s40729-017-0079-1>. PMID:28462508.
41. Gehrke SA, Marin GW. Biomechanical evaluation of dental implants with three different designs: removal torque and resonance frequency analysis in rabbits. *Ann Anat*. 2015;199:30-5. <http://doi.org/10.1016/j.aanat.2014.07.009>. PMID:25224495.
42. Seong WJ, Kim HC, Jeong S, DeVea DL, Aparicio C, Li Y, et al. Ex vivo mechanical properties of dental implant bone cement used to rescue initially unstable dental implants: a rabbit study. *Int J Oral Maxillofac Implants*. 2011;26(4):826-36. PMID:21841993.
43. Kang C-G, Park Y-B, Choi H, Oh S, Lee K-W, Choi S-H, et al. Osseointegration of Implants Surface-Treated with Various Diameters of TiO₂ Nanotubes in Rabbit. *J Nanomater*. 2015;2015:634650. <http://doi.org/10.1155/2015/634650>.
44. Hamad TI, Fatalla AA, Waheed AS, Azzawi ZGM, Cao YG, Song K. Biomechanical Evaluation of Nano-Zirconia Coatings on Ti-6Al-7Nb Implant Screws in Rabbit Tibias. *Curr Med Sci*. 2018;38(3):530-7. <http://doi.org/10.1007/s11596-018-1911-4>. PMID:30074223.
45. Larsson Wexell C, Thomsen P, Aronsson BO, Tengvall P, Rodahl M, Lausmaa J, et al. Bone response to surface-modified titanium implants: studies on the early tissue response to implants with different surface characteristics. *Int J Biomater*. 2013;2013:412482. <http://doi.org/10.1155/2013/412482>. PMID:24174936.
46. Lee JT, Cho SA. Biomechanical evaluation of laser-etched Ti implant surfaces vs. chemically modified SLA Ti implant surfaces: removal torque and resonance frequency analysis in rabbit tibias. *J Mech Behav Biomed Mater*. 2016;61:299-307. <http://doi.org/10.1016/j.jmbbm.2016.03.034>. PMID:27093590.
47. Yuan B, Cheng Q, Zhao R, Zhu X, Yang X, Yang X, et al. Comparison of osteointegration property between PEKK and PEEK: effects of surface structure and chemistry. *Biomaterials*. 2018;170:116-26. <http://doi.org/10.1016/j.biomaterials.2018.04.014>. PMID:29660634.
48. Olivares-Navarrete R, Hyzy SL, Gittens RA, Schneider JM, Haithcock DA, Ullrich PF, et al. Rough titanium alloys regulate osteoblast production of angiogenic factors. *Spine J*. 2013;13(11):1563-70. <http://doi.org/10.1016/j.spinee.2013.03.047>. PMID:23684238.
49. Chen WC, Chen YS, Ko CL, Lin Y, Kuo TH, Kuo HN. Interaction of progenitor bone cells with different surface modifications of titanium implant. *Mater Sci Eng C*. 2014;37:305-13. <http://doi.org/10.1016/j.msec.2014.01.022>. PMID:24582253.
50. Chen WC, Ko CL. Roughened titanium surfaces with silane and further RGD peptide modification in vitro. *Mater Sci Eng C Mater Biol Appl*. 2013;33(5):2713-22. <http://doi.org/10.1016/j.msec.2013.02.040>. PMID:23623088.
51. Monjo M, Petzold C, Ramis JM, Lyngstadaas SP, Ellingsen JE. In vitro osteogenic properties of two dental implant surfaces. *Int J Biomater*. 2012;2012:181024. <http://doi.org/10.1155/2012/181024>. PMID:23118752.
52. Rupp F, Gittens RA, Scheideler L, Marmur A, Boyan BD, Schwartz Z, et al. A review on the wettability of dental implant surfaces I: theoretical and experimental aspects. *Acta Biomater*. 2014;10(7):2894-906. <http://doi.org/10.1016/j.actbio.2014.02.040>. PMID:24590162.
53. West G, Kelly P. Influence of inert gas species on the growth of silver and molybdenum films via a magnetron discharge. *Surf Coat Tech*. 2011;206(7):1648-52. <http://doi.org/10.1016/j.surfcoat.2011.08.025>.
54. Schneider GB, Zaharias R, Stanford C. Osteoblast integrin adhesion and signaling regulate mineralization. *J Dent Res*. 2001;80(6):1540-4. <http://doi.org/10.1177/00220345010800061201>. PMID:11499509.
55. Genge BR, Sauer GR, Wu LN, McLean FM, Wuthier RE. Correlation between loss of alkaline phosphatase activity and accumulation of calcium during matrix vesicle-mediated mineralization. *J Biol Chem*. 1988;263(34):18513-9. [http://doi.org/10.1016/S0021-9258\(19\)81388-1](http://doi.org/10.1016/S0021-9258(19)81388-1). PMID:3192545.
56. Yan S, Komasa S, Agariguchi A, Pezzotti G, Okazaki J, Maekawa K. Osseointegration properties of titanium implants treated by nonthermal atmospheric-pressure nitrogen plasma. *Int J Mol Sci*. 2022;23(23):15420. <http://doi.org/10.3390/ijms232315420>. PMID:36499747.

Moamin I. Issa

(Corresponding address)

University of Baghdad, College of Dentistry, Department of Prosthodontics, Baghdad, Iraq.

Email: moamin_alniama@codental.uobaghdad.edu.iq

Date submitted: 2024 Jan 17

Accept submission: 2024 May 30